International Journal of Innovative Engineering Applications

Journal homepage: https://dergipark.org.tr/ijiea

COMPRESSION METHODS FOR SATELLITE IMAGES USING WAVELET TRANSFORM AND PERFORMANCE EVALUATION

İbrahim Öz*[1]

[1]*Ankara Yildirim Beyazit University, Technology Transfer Office, Ankara/ Turkey*

Abstract

Original scientific paper

Research on image compression spans various fields, focusing on achieving efficient compression while preserving a specific image quality. Satellite images captured by observation satellites possess unique characteristics distinct from other images. Analyzing these specific qualities is decisive, leading to the proposal of tailored compression methods and transforms suitable for satellite image characteristics. This study comprehensively assesses the performance of six well-known compression methods in the literature, utilizing wavelet transform and metrics such as bits per pixel (BPP), compression ratio (CR), Peak Signal-to-Noise Ratio (PSNR), calculation time (CT), and Mean Squared Error (MSE). The compressed satellite images, generated through six methods and the Coif3 wavelet, are systematically compared and evaluated using performance metrics. The average values obtained for all six methods are 96.37%, 47.10 dB, and 7.92 seconds for CR, PSNR, and CT receptively, while WDR exhibits CR at 96.36%, PSNR at 48.84 dB, and CT at 6.58 seconds. The findings indicate that the Wavelet Difference Reduction (WDR) compression method utilizing the Coif3 wavelet outperforms others when considering all parameters together. We suggest that operators and manufacturers choose wavelet transform and WDR compression methods for effective compression of observation satellite images to achieve optimal results.

Keywords:*Image compression, satellite image, suitable compression methods, wavelet transform.*

DALGACIK DÖNÜŞÜMÜ İLE UYDU GÖRÜNTÜSÜ SIKIŞTIRMA METOTLARI VE PERFORMANS DEĞERLENDİRMESİ

Özet

Orijinal bilimsel makale

Görüntü sıkıştırma üzerine birçok alanda araştırma yapılmakta ve hedef belirli bir görüntü kalitesini korurken iyi bir sıkıştırma oranı elde etmektir. Gözlem uyduları tarafından çekilen uydu görüntüleri, diğer görüntülerden farklı özelliklere sahiptir. Bu özelliklerin analizi ile bu alana özgü dönüşüm ve sıkıştırma teknikleri geliştirilebilir. Bu çalışmada uydu görüntüsü sıkıştırılmış, dalgacık dönüşümü ve literatürde çok bilinen altı sıkıştırma yönteminin performansı; piksel başına bit (PBB), sıkıştırma oranı (SO), tepe sinyal gürültü oranı (TSGO), hesaplama süresi (HS) ve ortalama kare hata (OKH) gibi ölçütler kullanarak kapsamlı bir şekilde değerlendirilmiştir. Coif3 dalgacık dönüşümü ve bu altı sıkıştırma metodu kullanılarak elde edilen sıkıştırılmış uydu görüntüsü sistematik olarak karşılaştırılırmış ve değerlendirilmiştir. Altı yöntemin ortalama değerleri SO için %96.37, TSGO için %47.10 db ve HS için7.92 saniye iken, WDR metodunda SO, %96.36, TSGO %48.34 db ve HS 6.58 saniye olarak elde edilmiştir. Bulgular, Coif3 dalgacık dönüşümü kullanan WDR sıkıştırma yönteminin, tüm performans parametreleri dikkate alındığında diğer yöntemleri geride bıraktığını göstermektedir. Bu çalışma sonuçlarına göre uydu operatörleri ve işletmecilerine gözlem uydusu görüntüsü sıkıştırma işleminde başarılı sonuçlarından dolayıdalgacık dönüşümü ve WDR metodunu öneriyoruz.

Anahtar Kelimeler: *Dalgacık dönüşümü, görüntü sıkıştırma, uydu görüntüsü, uygun sıkıştırma metotları.*

1 Introduction

Image compression is decisive in digital data processing and transmission, especially in scientific and technological fields. The need for image compression arises from various factors, including limitations in data storage, the demand for efficient transmission, and the need to optimize available resources. [1]. Scientifically, the utilization of image compression arises from several essential considerations. Firstly, the inherent challenge of limited storage capacity confronts scientific datasets, particularly those generated by sources like remote sensing satellites [2-5] or medical imaging devices. This results in the need to condense data without compromising crucial

*Corresponding author.

E-mail address: ibrahimoz@gazi.edu.tr (İ. Öz)

Received 21 February 2024; Received in revised form 20 September 2024; Accepted 16 December 2024

 Doi: https://doi.org/10.46460/ijiea.1440970

information [6, 7]. Moreover, bandwidth constraints pose challenges when transmitting large image files over networks with limited capacity, making compression essential for efficient data transmission. Resource optimization is another crucial aspect, as the computational and hardware resources necessary for processing extensive image data can be substantial, and compression aids in minimizing these demands. Compressed images facilitate swift data transfer and analysis in applications demanding real-time processing, such as medical diagnostics or satellite communication.

Additionally, image compression contributes to cost efficiency by mitigating expenses related to storage infrastructure and network resources. The preservation of information is a paramount concern during compression, with practical methods striving to retain critical scientific details and features within the compressed images. Lastly, in scientific endeavors like space exploration or environmental monitoring, where data is remotely collected, compression becomes indispensable for extracting relevant information while minimizing the impractical transmission of vast amounts of data back to Earth [8, 9].

Satellite imagery obtained through remote sensing technologies exhibits advancements in spatial, temporal, and spectral resolutions and increased data rates, as outlined in Table 1. This progression, however, results in escalating compression requirements due to the burgeoning wealth of information. Managing vast data volumes at each stage of the image acquisition process becomes a challenge, necessitating the application of compression techniques to streamline satellite image data [10 -12].

Table 1. Earth Observation Satellites and Technical Properties.

Satellites	Swath (km)	Spatial Resolution (m)	Data rate (Mbps)
Rasat	30	7.5/15	25
Gokturk 2	20	2.5/5	100
Göktürk 1	15	0.5/1	465
İmece	19	1/4	320
Spot 5	60	2.5	128
Quick Bird	18	2.6	320
Ikonos	11	3.2	320

The computational load posed by large multispectral imageries and concerns about data storage and transmission underscores the urgency of employing compression methods. While lossless compression ensures data volume reduction without information loss, it becomes indispensable given the significant expense and subsequent utilization of multispectral data for extensive analysis and processing operations, including classification and target detection. In scenarios where higher compression is acceptable, lossy image compression methods can be employed to balance data reduction and preserving essential information [13-15].

Satellite images, renowned for accurately mapping geospatial features, incur challenges such as high storage requirements, hardware throughput constraints, and the need for data transmission under limited bandwidth and time windows. These limitations necessitate the utilization of image compression algorithms to alleviate dependency on constraints. Various techniques have been explored, ranging from the Direct Cosine Transform (DCT) to more computationally efficient methods like the Bandelets transform [16].

Earth Observation (EO) satellites primarily utilize onboard multispectral imagers to acquire images, employing separate sensors for different wavelengths. Multispectral images, crucial in remote sensing applications, face challenges due to the limited capabilities of onboard satellite hardware. Image compression becomes imperative to reduce onboard data storage and transmission bandwidth requirements, especially during the satellite's limited passes over ground stations. Increasing the compression ratio emerges as a primary goal to optimize resource utilization while preserving scientific information during image reconstruction on Earth [11, 17,18].

Recent studies in satellite image compression methods and performance evaluation highlight the ongoing advancements in the field. For instance, the Lightweight Bit-Depth Recovery Network for Gaofen Satellite Multispectral Image Compression [19] explores efficient recovery techniques for multispectral images, addressing the challenges of bit-depth reduction. The study Satellite Image Compression and Denoising with Neural Networks [3] leverages neural network architectures to simultaneously compress and denoise satellite imagery, demonstrating the potential of AI-driven approaches. The research on a Computationally Efficient Compression Scheme for Satellite Images [16] focuses on optimizing computational resources while maintaining image quality, catering to the constraints of onboard processing. Additionally, the study titled Efficient Onboard Compression for Arbitrary-Shaped Cloud-Covered Remote Sensing Images via Adaptive Filling and Controllable Quantization [20] introduces innovative techniques for handling complex image geometries, including cloud-covered areas, through adaptive filling and precise quantization strategies. These recent works emphasize the evolving nature of satellite image compression, aiming to improve efficiency, quality, and applicability in various remote sensing scenarios.

The spectrum of image compression schemes falls into two main categories: lossless and lossy. While lossless compression, exemplified by the CCSDS 123 algorithm, maintains information integrity, lossy compression, such as JPEG2000, accepts a controlled amount of data loss for significantly higher compression ratios. In this context, DWT-based compression techniques gain prominence over DCT-based methods, offering multi-resolution transforms and achieving superior compression ratios with enhanced reconstructed image quality [13, 22-24].

Notably, some satellite missions, including Mars Exploration Rover, Rasat, X-Sat, and Pleiades-HR, demonstrate the prevalence of wavelet-based compression techniques in handling payloads. This underscores the applicability of such methods in the developing landscape of satellite technology.

2 Wavelet Transform and Compression Methods

The wavelet transform is a versatile tool with applications in diverse fields, including fault detection, medical applications, and crop recognition [23, 27- 30]. Its relevance continues to grow, making it an emerging field of study.

Wavelet-based image compression is a process where individual images are transformed and analyzed. The wavelet transform breaks down an image into its frequency components, creating a multi-resolution representation. This transformation is effective for compression as it eliminates unnecessary or less noticeable image data while keeping important visual information intact. The process involves several steps, starting with the application of wavelet transforms and progressing through quantization and, coding i.e., Progressive Coefficients Significance Methods (PCSM), ultimately resulting in the creation of a compressed image, as depicted in Figure 1.

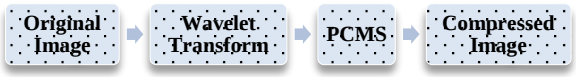

Figure 1. Basics steps of image compression: Transform, Quantization, and Coding (PCMS).

The first step involves the transformation of the image, where it undergoes decomposition into wavelet coefficients. This process is typically executed using techniques like the discrete wavelet transform (DWT) or the lifting scheme. Composing the image in this manner enables extracting key features and details.

Following the transformation, the next step is quantization. During this stage, the coefficients obtained from the wavelet transformation are quantized. Higher frequency and less perceptually significant coefficients are subjected to more aggressive quantization. This step is crucial in prioritizing and preserving essential image information while efficiently managing data size.

The final step in wavelet-based image compression is entropy coding. This involves the application of coding techniques such as Huffman coding or arithmetic coding. The primary objective here is to compress the quantized coefficients further, optimizing the storage and transmission of the compressed image [31, 32].

Collectively, these steps form a systematic approach to wavelet-based image compression, demonstrating its effectiveness in various applications. This process reduces data size and ensures the retention of critical image details, making it a valuable technique in fields requiring efficient data management and transmission.

In the specific domain of wavelet-based image compression, a series of sequential steps are employed to achieve efficient data reduction. Satellite image compression is essential for optimizing storage and transmission bandwidth without compromising crucial information,

2.1 Overview of Coif3 Wavelet

The Coif3 wavelet, short for Coiflet-3, belongs to the Coiflets family, a class of wavelets designed to balance smoothness and vanishing moments. The Coif3 wavelet, in particular, possesses three vanishing moments, providing effective localization in both time and frequency domains. The scaling function, responsible for generating a Coiflet, is formulated as the solution to the scaling equation [29, 30].

$$\psi(x) = \sum_{k=2-N}^{1} (-1)^k a_{1-k} \phi(2x-k) \quad (1)$$

where the ϕ scaling coefficients are selected to ensure that the associated scaling functions and wavelets have the necessary properties.

The Coif3 wavelet's three vanishing moments ensure that the wavelet function cancels out polynomials of degree two. This property aids in capturing and representing details in the signal effectively [32].

$$\phi(x) = 2 \sum_{k \epsilon Z} h_k \phi(2x-k) \quad (2)$$

The scaling coefficients h_k are determined to ensure that the corresponding scaling functions and wavelets possess the necessary properties.

Figure 2 represents Coif3 wavelet functions. Coif3 wavelet is orthogonal, forming a complete and orthonormal basis for representing signals. Orthogonality simplifies computations and ensures energy preservation during the transformation process.

Coif3 wavelet balances regularity and smoothness, making it well-suited for applications where preservation of fine details is crucial, such as in image compression.

The Coif3 wavelet's characteristics contribute to an effective and balanced decomposition, ensuring that both high and low-frequency details are appropriately represented.

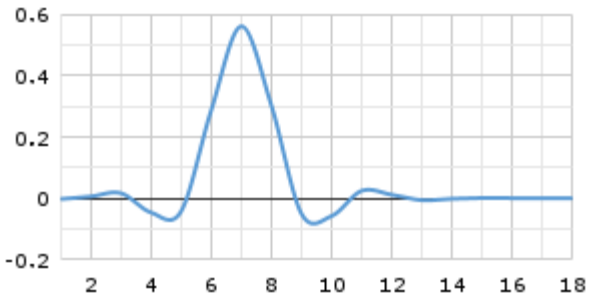

Figure 2. Coif3 wave function.

We chose the Coif3 wavelet based on the outcomes of the PhD dissertation titled 'Image and Video Compression Using Two-Dimensional Wavelet Transform' [24]. In our study, we implemented the Coif3 wavelet with a 4-level decomposition in our compression methods. Opting for higher decomposition levels enhances image quality. To strike a balance and address concerns like computation time, we specifically chose a 4-level decomposition for our research. This process involves breaking the image into wavelet coefficients, representing various frequency components. Following the approach outlined in the mentioned thesis, for Huffman coding with a compression ratio of 10 applied to a standard house image, the PSNR values are 35.10, 36.71, 36.94, and 39.99 dB for

decomposition levels 1, 2, 3, and 4, respectively. Notably, all methods in our study incorporate the Coif3 wavelet transform during the compression process. This decision is made to balance computational efficiency and the ability to capture details present in the image [24].

Figure 3 presents a detailed representation of a four-level decomposition of the test satellite images. Using the Coif3 wavelet, this process carefully breaks down the image into different components, capturing the overall structure and finer details. The result includes approximation and detailed coefficients covering horizontal, diagonal, and vertical components. This multi-level decomposition is essential for gaining insights into the intrinsic characteristics of satellite imagery.

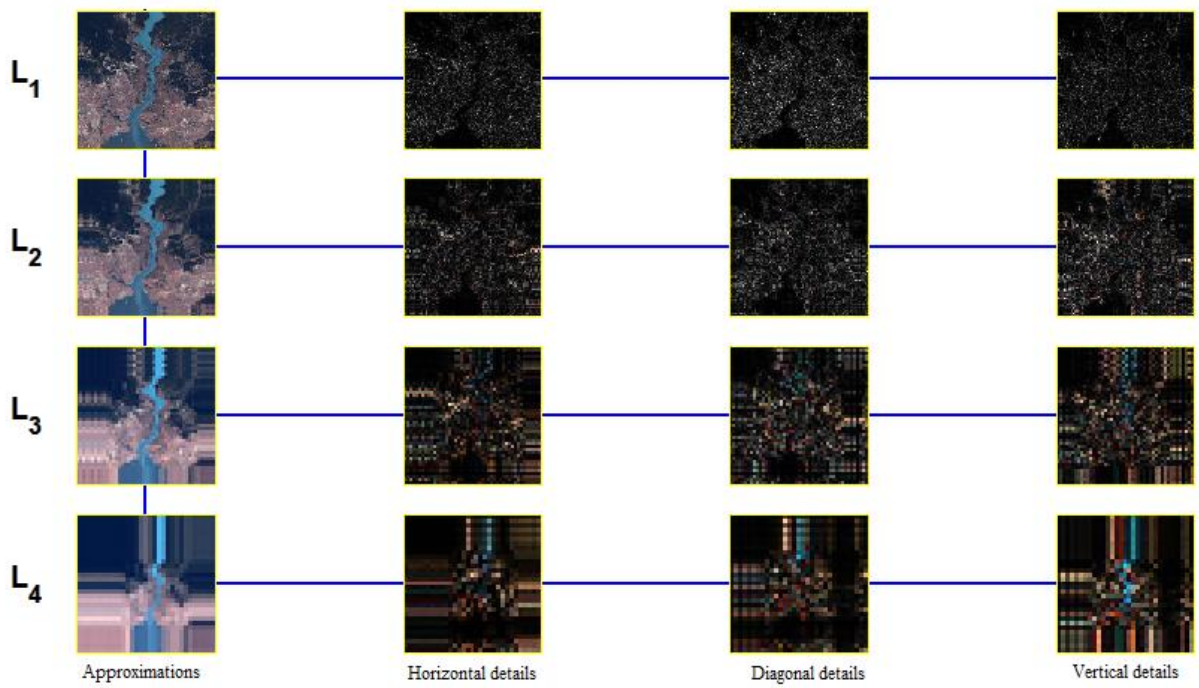

Figure 3. Four-level image decomposition and approximations, horizontal details, diagonal details and vertical details for each level.

The acquired coefficients undergo a crucial phase in the analytical process in the next step. Six distinct compression methods are systematically applied to these coefficients, aiming to evaluate and compare the efficiency of each method. This meticulous analysis delves into how well these compression techniques handle the diverse and intricate information embedded within the coefficients. By scrutinizing the compressed results, we gain valuable insights into the methods' ability to reduce data without sacrificing the essential features and nuances in the satellite images. The intricate dance between Coif3 wavelet decomposition and subsequent compression methods unfolds, shedding light on optimizing storage and transmission while preserving the scientific significance of satellite imagery.

2.2 Methods to Compress Satellite Image

This study thoroughly evaluated the effectiveness of six widely recognized Progressive Coefficients Significance Methods (PCSM), based on an extensive analysis [33]. These six methods were intentionally selected due to their broad popularity in the literature, especially in image compression and other related applications [34-36]. The raw satellite images used in this research were sourced from Rasat EO satellites, further emphasizing the relevance of these methods for satellite image compression.

2.2.1 Embedded Zero Tree Wavelet (EZW)

The Embedded Zero Tree Wavelet algorithm (EZW) is a valuable image compression technique that generates a fully embedded bit stream for image coding. Remarkably competitive in compression performance with known techniques, this method requires no training, pre-stored codebooks, or prior image source knowledge. EZW is rooted in four fundamental concepts: discrete wavelet transform (DWT) or hierarchical sub-band decomposition, prediction of information absence across scales, entropy-coded successive-approximation quantization, and universal lossless data compression through adaptive arithmetic coding. The algorithm's consecutive operation is noteworthy, ceasing upon meeting a target bit rate or distortion. The encoding process represents a pivotal aspect of EZW.

2.2.2 Set-Partitioning In Hierarchical Trees (SPIHT):

SPIHT is a fully embedded wavelet coding algorithm prioritizing information in decreasing energy levels. It allocates the bit budget between encoding the tree map and the significance information, enabling precise rate control and reasonable computational complexity. Reportedly surpassing other coding techniques like DCT and EZT, SPIHT, an enhanced version of EZW, has demonstrated superior performance with high PSNR values for diverse images. Its widespread adoption makes it a standard for

comparing subsequent wavelet-based image compression algorithms.

2.2.3 Spatial-Orientation Tree Wavelet (STW)

STW is essentially an adaptation of the SPIHT algorithm, differing only in the organization of coding output. It utilizes a state transition model to encode zero tree information, deviating from EZW's approach. The 3D_spiht scheme, an extension from 2D SPIHT, maintains partial ordering by magnitude, ordered bit-plane transmission, and the SPIHT algorithm's principles.

2.2.4 Wavelet Difference Reduction (WDR)

The WDR algorithm is a straightforward procedure involving a wavelet transform applied to the image, followed by bit-plane-based WDR encoding for the wavelet coefficients.

2.2.5 Adaptively Scanned Wavelet Difference Reduction (ASWDR)

ASWDR is a generalization of the WDR method by Tian and Wells, producing an embedded bit stream for progressive transmission and encoding precise indices for significant transform values. This capability facilitates Region of Interest (ROI) and various image processing operations on compressed image files [12].

2.2.6 SPIHT_3D

SPIHT_3D exploits self-similarity across spatial-temporal orientation trees, providing a wholly-embedded compressed bit stream. This characteristic allows for progressive video quality, enabling the algorithm to stop at any compressed file size or run until nearly lossless reconstruction. Such flexibility is desirable in applications like high-definition television.

2.3 Evaluation Metrics

In this study, we employ the following evaluation metrics to assess the performance of the compression methods applied to satellite images [33, 34].

2.3.1. Bit Per Pixel (bpp)

Bpp is a fundamental metric representing the average number of bits required to encode each pixel in the compressed image. It provides insights into the overall efficiency of the compression methods regarding data representation.

$$bpp = \frac{n*8}{H*W} \quad (4)$$

where H: the height of an image, W: the width of an image.

2.3.2. Compression Ratio

The compression ratio measures the extent to which the image size is reduced after compression. It is calculated as the ratio of the original image size to the compressed image size.

$$CR = \left(1 - \frac{h_c}{h_i}\right) * 100 \quad (5)$$

where, h_c: the number of bits in the compressed image, h_i: the number of bits in the original image.

2.3.3. Mean Squared Error (MSE)

MSE represents the average squared difference between the original and compressed images. Lower MSE values indicate better fidelity in image reconstruction.

$$MSE = \frac{1}{mn}\sum_{i=0}^{m=1}\sum_{j=0}^{n=1}|X(i,j) - X_c(i.j)|^2 \quad (6)$$

where M and N represent the image's size, X represents the given input image and X_c represents the reconstructed image.

2.3.3. Peak Signal-to-Noise Ratio (PSNR)

PSNR quantifies the quality of the compressed image by comparing it to the original. Higher PSNR values indicate better preservation of image quality.

$$PSNR = 10log_{10}(\frac{max^2}{MSE}) \quad (7)$$

where max : the maximum possible pixel value of the image.

2.3.5. Calculation Time

The time taken by each compression method for processing is a critical factor, especially in real-time applications. It provides insights into the computational efficiency of the methods.

$$CT = cpu_{t2} - cpu_{t1} \quad (8)$$

where cpu_{t2}: process stop time, cpu_{t1}: process start time.

A satellite test image showcasing diverse characteristics served as the focal point for our analysis. Employing the Coif3 wavelet during the transform phase, we applied six compression methods to compress the image. Subsequently, the resultant images underwent evaluation using predefined metrics.

Systematic comparisons were made among the outcomes of each compression method, relying on evaluation metrics such as bits per pixel (bpp), compression ratio, Peak signal-to-noise ratio (PSNR), Mean Squared Error (MSE), and calculation time. This comprehensive assessment provided insights into the performance of each method across these criteria.

The results derived from the satellite images were compared with those obtained from a standard test image commonly employed in compression studies to verify our findings. This comparative analysis further validated the effectiveness and reliability of our compression methods in handling satellite image data.

3 Results and Discussion

In this study, we carefully compressed a satellite test image using six distinct compression methods. We specifically chose the Coif3 wavelet for the transformation phase due to its exceptional performance, seamlessly meeting the study's requirements. The decision to use Coif3 is rooted in its proven effectiveness in balancing detail capture and computational efficiency. The assessment is conducted based on key statistical parameters such as bits per pixel (BPP), compression ratio (CR), Peak signal-to-noise ratio (PSNR), calculation time, and Mean Squared Error (MSE).

Figure 4 presents the results of satellite image compression using six analyzed compression methods, considering different numbers of encoding loops. It is important to note that the Coif3 wavelet transformer remains constant across all scenarios. Figure 4a illustrates the compression methods bit-per-pixel (bpp) performances. Notably, the WDR method achieves the best values, and the SP-3D method exhibits the lowest curve. Figure 4b provides insights into the calculation time, with the SPIHT method demonstrating the most efficient performance among the methods.

In contrast, the EZW method lags behind with the least favorable results. Figures 4c and 4d depict the peak signal-to-noise ratio (PSNR) and compression ratio (CR) performances, respectively. The WDR method yields higher PSNR, while three other methods demonstrate comparable results. Regarding compression ratio, the WDR method excels, offering the most efficient compression, whereas the SP-3D method exhibits the least favorable results.

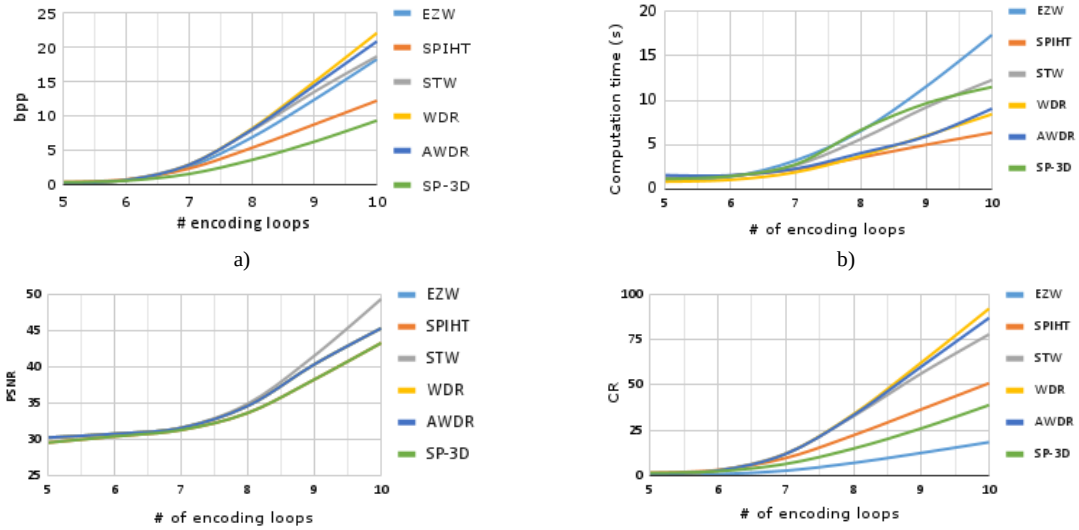

Figure 4. Satellite image compression performances using six methods from 5 to 10 encoding loops a) bit per pixel b) calculations time c) image quality, PSNR d) compression ratio.

Within Figure 5, a visual narrative unfolds, presenting a triptych of images that encapsulate the transformative journey of a test satellite image. The pristine satellite image on the left stands as the original, untouched representation. In the center, we witness the intricate web of details unveiled through the original decomposition process, showcasing the distinct components obtained through the Coif3 wavelet family. Finally, on the right emerges the reconstructed image, a harmonious synthesis achieved through the marriage of Coif3 wavelet decomposition and the WDR compression method, meticulously executed across 10 encoding loops.

In this scenario, utilizing the Coif3 wavelet family and the WDR compression method reveals a result adorned with a remarkable 45 dB PSNR (Peak Signal-to-Noise Ratio) value. This metric, indicative of the fidelity between the original and reconstructed images, underscores the method's proficiency in retaining crucial information during the compression process. Furthermore, the Compression Ratio (CR) of 8% highlights the adeptness of the chosen compression strategy in significantly reducing data size while maintaining a balance that allows for efficient storage and transmission.

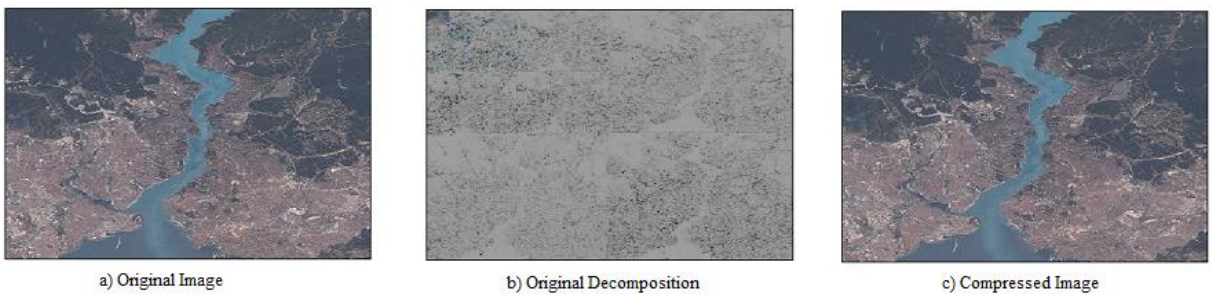

Figure 5. a) Original satellite image b) four-level wavelet decomposition c) reconstructed image.

These visual and quantitative insights provide a captivating glimpse into the transformative capabilities of the Coif3 wavelet family and the WDR compression method, showcasing their collaborative prowess in striking a harmonious balance between preservation and efficiency in the realm of satellite image processing.

Table 2 presents the statistical results of satellite image compression employing various compression methods for encoding loops ranging from 5 to 10. Notably, the WDR method attains the best bit per pixel (bbp) value at 15.62 bpp, displaying its efficiency in data representation. The highest compression ratio (CR) is achieved using the EZW method, reaching an impressive 96.55 db. In terms of peak signal-to-noise ratio (PSNR), the WDR method excels, attaining the highest value at 48.85. Similarly, the mean squared error (MSE) is optimal for the WDR, EZW, and ASWDR methods, all obtaining the best MSE at 35.51. Furthermore, the WDR method stands out for its computational efficiency, boasting the lowest computation time at 6.58 seconds in 10 loops, emphasizing its effectiveness in achieving a balance between compression performance and computational speed.

The overall performance of compression methods can be expressed as;

$$P_{all} = CR + PSNR + (CT_{max} - CT) \quad (9)$$

WDR demonstrates superior overall performance, achieving a value of 152.34, as illustrated in the last row of Table 2.

Table 2. Performance values of Satellite Image Coif3 Transform and Six Compression Methods.

	EZW		SP		STW		WDR		ASWDR		SP3D	
	max	Average	max	Average	max	Average	max	Average	max	Average	max	Average
bpp	13.32	5.26	6.59	2.94	9.29	3.44	15.62	6.08	15.06	5.96	5.32	2.33
CR	96.55	78.07	95.46	87.76	97.05	85.69	96.36	74.68	96.28	75.19	96.50	90.29
PSNR	48.34	40.07	44.45	35.52	48.65	37.81	48.84	40.07	48.34	40.07	44.45	35.52
CT	13.72	6.40	5.47	2.90	7.13	3.49	6.58	2.85	7.75	3.50	6.86	3.67
MSE	36.51	12.87	107.64	35.80	58.92	21.99	36.51	12.87	36.51	12.87	107.64	35.80
P_{all}	144.89	125.47	148.16	134.11	152.29	133.73	152.34	125.63	150.59	125.49	117.35	135.87

It is crucial to ensure satisfaction with the results by comparing them with established references. Therefore, for the purpose of comparative analysis, the results obtained from WDR are compared with those from the well-known Huffman coding.

Table 3 presents a comprehensive comparative analysis of compression performance for satellite images, utilizing both Huffman coding (huf_lvl) and Wavelet Difference Reduction (WDR) techniques. The satellite images undergo Coif3 wavelet decomposition at level 4, and various statistical parameters are assessed by selecting the number of encoding loops from 5 to 10 in compression methods to evaluate their effectiveness.

In the case of Huffman coding, the bits per pixel (BPP) range from a minimum of 0.66 to a maximum of 14.00, with an average of 8.35, indicating variations in data representation. Compression ratios (CR) range from 41.68 to 97.25, with an average of 65.22, significantly reducing data size. Peak Signal-to-Noise Ratio (PSNR) values vary between 31.00 and 48.74, with an average of 39.94, reflecting the quality of the compressed images. The computational efficiency is evident in the calculation time, ranging from 0.41 to 3.28 seconds, with an average of 1.85 seconds. Mean Squared Error (MSE) values range from 0.87 to 51.71, averaging 14.73, representing the deviation between the original and compressed images.

On the other hand, Wavelet Difference Reduction (WDR) outperforms in bits per pixel (BPP), with a range of 0.87 to 15.62 and an average of 6.08, displaying its efficiency in data representation. Compression ratios (CR) for WDR vary between 34.93 and 96.36, with an average of 74.68, indicating a substantial reduction in data size. PSNR values for WDR range from 32.51 to 48.34, averaging at 40.07, highlighting the method's proficiency in preserving image quality. WDR also demonstrates computational efficiency, with calculation times ranging from 1.08 to 6.58 seconds and an average of 2.85 seconds. MSE values for WDR span from 0.95 to 36.51, averaging 12.87, emphasizing the accuracy of the compressed images.

In terms of overall performance, the Huffman coding method scores 149.29, while the WDR technique achieves a slightly lower value of 144.70. These values are indicative of the effectiveness of the respective compression methods when considering multiple performance metrics

This comprehensive comparison offers nuanced insights into the performance of Huffman coding and Wavelet Difference Reduction. It provides a detailed understanding of their strengths and limitations across key statistical parameters in satellite image compression.

Table 3 Performance Comparison of Satellite Image with Coif3 Transform and Decomposition Level-4: Huffman vs. WDR.

	Huffman			WDR		
	max	min	avg	max	min	Average
bpp	14.00	0.66	8.35	15.62	0.87	6.08
CR	97.25	41.68	65.22	96.36	34.93	74.68
PSNR	48.74	31.00	39.94	48.84	32.51	40.07
CT	3.28	0.41	1.85	6.58	1.08	2.85
MSE	51.71	0.87	14.73	36.51	0.95	12.87
P_{all}	149.29	78.85	109.90	144.70	72.94	118.49

A well-known daily house image was selected for evaluation to assess the performance of Wavelet Difference Reduction (WDR) in satellite image compression. Both images were compressed by employing WDR and Huffman methods while maintaining the Coif3 wavelet transform.

Table 4 comprehensively compares compression performances for daily house images using Huffman coding and Wavelet Difference Reduction (WDR) techniques. The house images undergo Coif3 wavelet decomposition at level 4, and various statistical parameters are evaluated to assess the efficiency of the compression methods.

For Huffman coding, the bits per pixel (BPP) values range from a minimum of 1.34 to a maximum of 11.66, with an average of 6.87, illustrating variations in data representation. Compression ratios (CR) range from 51.43 to 94.43, with an average of 71.39, indicating a substantial reduction in data size. Peak Signal-to-Noise Ratio (PSNR) values vary between 36.42 and 54.67, with an average of 47.02, reflecting the quality of the compressed images. The computational efficiency is evident in the calculation time, ranging from 0.50 to 3.11 seconds, with an average of 1.88 seconds. Mean Squared Error (MSE) values range from 0.22 to 14.84, with an average of 3.07, representing the deviation between the original and compressed images.

On the other hand, Wavelet Difference Reduction (WDR) outperforms in bits per pixel (BPP), with a range of 0.35 to 9.86 and an average of 3.40, displaying its efficiency in data representation. Compression ratios (CR100) for WDR vary between 58.92 and 98.54, with an average of 85.85, indicating a substantial reduction in data size. PSNR values for WDR range from 31.22 to 45.00, averaging at 37.19, highlighting the method's proficiency in preserving image quality. WDR also demonstrates computational efficiency, with calculation times ranging from 0.84 to 3.22 seconds and an average of 1.56 seconds. MSE values for WDR span from 2.05 to 49.05, averaging at 20.22, emphasizing the accuracy of the compressed images.

Table 4 Performance Comparison of House Image with Coif3 Transform and Decomposition Level-4: Huffman vs. WDR.

	Huffman			WDR		
	max	min	avg	max	min	Average
bpp	11.66	1.34	6.87	9.86	0.35	3.40
CR	94.43	51.43	71.39	98.54	58.92	85.85
PSNR	54.67	36.42	47.02	45.00	31.22	37.19
CT	3.11	0.50	1.88	3.22	0.84	1.56
MSE	14.84	0.22	3.07	49.05	2.05	20.22
P_{all}	152.54	93.90	123.08	146.87	95.85	128.03

Considering the overall performances of all compression methods, the Huffman coding method exhibits a commendable score of 152.54, highlighting its effectiveness in various aspects. On the other hand, the Wavelet Difference Reduction (WDR) method performs admirably with a slightly lower yet competitive score of 146.87. These values reflect the comprehensive assessment of both techniques across multiple performance metrics, demonstrating their respective strengths and capabilities in the context of image compression

The analysis of compression performance for both daily house and satellite images using Huffman coding and Wavelet Difference Reduction (WDR) techniques, as depicted in Tables 3 and Table 4, provides valuable insights into the effectiveness of these methods.

The Coif3 wavelet, known for combining smoothness and vanishing moments, is a valuable tool for transforming the satellite test image, capturing both spatial and spectral features. This intentional choice aims to enhance the efficiency and quality of the compression process, aligning with a systematic and informed approach. The study seeks to leverage the strengths of Coif3 to derive optimal insights and results from the compression methods employed.

The comparative analysis highlights the nuanced performance characteristics of Huffman coding and WDR when dealing with distinct image datasets. While Huffman coding demonstrates computational efficiency and competitive CR values, WDR excels in achieving lower BPP values, superior accuracy (reflected in lower MSE values), and competitive CR values. The selection between these methods would depend on the specific requirements and priorities of the given application, balancing considerations of data size reduction, computational efficiency, and image quality preservation.

4 Conclusion

This study evaluated the performance of six widely recognized compression methods specifically designed for satellite images. It acknowledged the unique characteristics of satellite imagery, which differ from other types of images, such as medical or everyday photos, each requiring distinct measurement metrics. The research aimed to demonstrate the impact of compression methods on satellite images while consistently utilizing the Coif3 wavelet as the transform. Key statistical parameters, including BPP, CR, PSNR, CT, and MSE, were analyzed to gain a comprehensive understanding of the strengths and limitations of each method.

WDR demonstrates superior accuracy in image reconstruction when considering all parameters together. The validation using the well-known Huffman coding further confirms the efficacy of the proposed WDR method.

Future endeavors in this research domain could focus on several promising directions. Firstly, exploring hybrid compression approaches that combine the strengths of Huffman coding and WDR could potentially yield enhanced results. Investigating the impact of varying wavelet families and decomposition levels on compression outcomes may provide valuable insights into optimizing the process further. Additionally, incorporating machine-learning techniques for adaptive compression based on image content and context could be an avenue for future exploration.

Further research efforts may also address the development of real-time compression algorithms for dynamic image data and explore the application of these compression methods in various domains, such as medical

imaging or video compression. Assessing the robustness of the compression methods under different image characteristics and exploring their performance on large-scale datasets could contribute to a more comprehensive understanding of their applicability.

In summary, the findings from this study lay the groundwork for future investigations that aim to refine existing compression methodologies, explore hybrid approaches, and adapt compression techniques to diverse and dynamic imaging scenarios. As technology advances and the demand for efficient image processing grows, continuous exploration and refinement of compression methods remain imperative for addressing evolving requirements in various scientific and technological domains.

Declaration

Ethics committee approval is not required.

References

[1] Othman, G., & Zeebaree, D. Q. (2020). The Applications of Discrete Wavelet Transform in Image processing: A review. *Journal of soft computing and data mining*, 1(2), 31-43.

[2] Indradjad, A., Nasution, A. S., Gunawan, H., & Widipaminto, A. (2019). A comparison of Satellite Image Compression methods in the Wavelet Domain. *In IOP Conference Series: Earth and Environmental Science* (Vol. 280, No. 1, p. 012031). IOP Publishing.

[3] De Oliveira, V. A., Chabert, M., Oberlin, T., Poulliat, C., Bruno, M., Latry, C., ... & Camarero, R. (2022). Satellite Image Compression and Denoising with Neural Networks. *IEEE Geoscience and Remote Sensing Letters*, 19, 1-5.

[4] Delaunay, X., Chabert, M., Charvillat, V., & Morin, G. (2010). Satellite Image Compression by Post-Transforms in the Wavelet Domain. *Signal processing*, 90(2), 599-610.

[5] Teke, M. (2016). Satellite Image Processing Workflow for RASAT and Göktürk-2. *Journal of Aeronautics and Space Technologies*, *9*(1), 1-13.

[6] Taş, İ. Ç. Application of Panoramic Dental X-Ray Images Denoising. International *Journal of Innovative Engineering Applications*, 7(1), 13-20.

[7] Toraman, S., & Turkoglu, I. (2020). Using Wavelet Transform and Machine Learning Techniques, a Wew Method for Classifying Colon Cancer Patients and Healthy People from FTIR Signals. *Journal of the Faculty of Engineering and Architecture of Gazi University*, 35(2), 933-942.

[8] Vura, S., Patil, P., & Patil, S. B. (2023). A Study of Different Compression Algorithms for Multispectral Images. Materials Today: *Proceedings*, *80*, 2193-2197.

[9] Kitaeff, V. V., Cannon, A., Wicenec, A., & Taubman, D. (2015). Astronomical Imagery: Considerations for a Contemporary Approach with JPEG2000. *Astronomy and Computing*, *12*, 229-239.

[10] Ma, X. (2023). High-resolution Image Compression Algorithms in Remote Sensing Imaging. *Displays*, 102462.

[11] Yu, G., Vladimirova, T., & Sweeting, M. N. (2009). Image Compression Systems on Board Satellites. *Acta Astronautica*, *64*(9-10), 988-1005.

[12] Liao, L., Xiao, J., Li, Y., Wang, M., & Hu, R. (2020). Learned Representation of Satellite Image Series for Data Compression. Remote Sensing, 12(3), 497.

[13] Shihab, H. S., Shafie, S., Ramli, A. R., & Ahmad, F. (2017). Enhancement of Satellite Image Compression Using a Hybrid (DWT–DCT) Algorithm. *Sensing and Imaging*, 18, 1-30.

[14] Swetha, V., Patil, G. P., & Patil, B. S. (2021, July). Lossless Compression of Satellite Images using a Versatile Hybrid Algorithm. *In IOP Conference Series: Materials Science and Engineering* (Vol. 1166, No. 1, p. 012048). IOP Publishing.

[15] Bacchus, P., Fraisse, R., Roumy, A., & Guillemot, C. (2022, July). Quasi Lossless Satellite Image Compression. In IGARSS 2022-2022 *IEEE International Geoscience and Remote Sensing Symposium* (pp. 1532-1535). IEEE.

[16] Jamuna Rani, M., & Azhagu Jaisudhan Pazhani, A. (2022). Computational Efficient Compression Scheme for Satellite Images. *Earth Science Informatics*, *15*(3), 1723-1736.

[17] Faria, L. N., Fonseca, L. M., & Costa, M. H. (2012). Performance Evaluation of Data Compression Systems Applied to Satellite Imagery. *Journal of Electrical and Computer Engineering*, 2012, 18-18.

[18] Hagag, A., Hassan, E. S., Amin, M., Abd El-Samie, F. E., & Fan, X. (2017). Satellite Multispectral Image Compression Based on Removing Sub-bands. *Optik*, 131, 1023-1035.

[19] Zhang, W., Li, D., Zhang, H., Yu, P., & Gao, W. (2024). Lightweight Bit-Depth Recovery Network for Gaofen Satellite Multispectral Image Compression. *IEEE Journal of Selected Topics in Applied Earth Observations and Remote Sensing*.

[20] Wang, K., Jia, J., Zhou, P., Ma, H., Yang, L., Liu, K., & Li, Y. (2024). Efficient Onboard Compression for Arbitrary-Shaped Cloud-Covered Remote Sensing Images via Adaptive Filling and Controllable Quantization. *Remote Sensing*, 16(18).

[21] Yilmaz, Ö., Aksoy, M., Kesilmiş, Z. (2019). Misalignment Fault Detection by Wavelet Analysis of Vibration Signals. *International Advanced Researches and Engineering Journal*, *3*(3), 156-163.

[22] Oz, I., Oz, C., Yumusak, N. (2001) Image Compression Using 2-D Multiple-Level Discrete Wavelet Transform (DWT). *Eleco 2001 International Conference on Electrical and Electronics Engineering*, Turkey

[23] Akmaz, D. (2022). Recognition Of Power Quality Events Using Wavelet Transform, K-Nearest Neighbor Algorithm And Gain Ratio Feature Selection Method. *International Journal of Innovative Engineering Applications*, *6*(1), 42-47.

[24] Oz, I.(2006). *Image and Video Compression by Using Two Dimensional Wavelet Transform* (Doctoral dissertation, Sakarya University).

[25] Saken, M., Yağci, M. B., & Yumuşak, N. (2021). Impact of Image Segmentation Techniques on Celiac Disease Classification Usingscale Invariant Texture Descriptors for Standard Flexible Endoscopic Systems. *Turkish Journal of Electrical Engineering and Computer Sciences*, 29(2), 598-615.

[26] Coşkun, M., Gürüler, H., Istanbullu, A., Peker, M. (2015). Determining the Appropriate Amount of Anesthetic Gas Using DWT and EMD Combined with Neural Network. *Journal of medical systems*, 39, 1-10.

[27] Coşkun, M., & İstanbullu, A. (2012). EEG İşaretlerinin FFT ve Dalgacık Dönüşümü ile Analizi. XIV. *Akademik Bilişim Konferansı*, Uşak, Türkiye.

[28] Akay, M., & Tuncer, T. (2021). Çok Seviyeli Dalgacık Dönüşümü ve Yerel İkili Örüntüler Tabanlı Otomatik EEG Duygu Tanıma Yöntemi. *International Journal of Innovative Engineering Applications*, 5(2), 75-80.

[29] Şengür, A., Türkoğlu, İ., & Ince, M. C. (2006). A Comparative Study on Entropic Thresholding Methods. *IU-Journal of Electrical & Electronics Engineering*, 6(2), 183-188.

[30] Yumusak, N., Temurtas, F., Cerezci, O., & Pazar, S. (1998, August). Image thresholding using measures of fuzziness. In IECON'98. *Proceedings of the 24th Annual Conference of the IEEE Industrial Electronics Society* (Cat. No. 98CH36200) (Vol. 3, pp. 1300-1305). IEEE.

[31] Černá, D., Finěk, V., & Najzar, K. (2008). On the exact values of coefficients of coiflets. *Open Mathematics*, *6*(1), 159-169.

[32] Taher, M. M., & Redha, S. M. (2022). Use The Coiflets and Daubechies Wavelet Transform To Reduce Data Noise For a Simple Experiment. *Iraqi Journal of Statistical Sciences*, *19*(2), 91-103.

[33] Kumar, R., & Singh, S. (2014). Comparative Analysis of Wavelet Based Compression Methods. *International Journal of Computer Networking, Wireless and Mobile Communications*, 143-150.

[34] Oz, I. (2024). Comparative Analysis of Wavelet Families in Image Compression, Featuring the Proposed New Wavelet. *Turkish Journal of Science and Technology*, 19(1), 279-294. https://doi.org/10.55525/tjst.1428424

[35] Marangoz, A. M., Sefercik, U. G., & Damla, YÜCE, (2020). Three-dimensional earth modelling performance analysis of Gokturk-2 satellite. *Turkish Journal of Engineering*, *4*(3), 164-168.

[36] Wang, K., Jia, J., Zhou, P., Ma, H., Yang, L., Liu, K., & Li, Y. (2024). Efficient Onboard Compression for Arbitrary-Shaped Cloud-Covered Remote Sensing Images via Adaptive Filling and Controllable Quantization. *Remote Sensing*, 16(18).